Mon. Not. R. astr. Soc. (1992) **258,** 749–758

# A new, EUV-bright intermediate polar discovered in the *ROSAT* Wide Field Camera all-sky survey

K. O. Mason,[1] M. G. Watson,[2] T. J. Ponman,[3] P. A. Charles,[4] S. R. Duck,[3] B. J. M. Hassall,[5] S. B. Howell,[6] M. Ishida,[7] D. H. P. Jones[5] and J. P. D. Mittaz[1]

[1] *Mullard Space Science Laboratory, University College London, Holmbury St Mary, Dorking, Surrey RH5 6NT*
[2] *Physics and Astronomy Department, University of Leicester, Leicester LE1 7RH*
[3] *School of Physics and Space Research, University of Birmingham, PO Box 363, Birmingham B15 2TT*
[4] *Royal Greenwich Observatory, Apartado 321, 38780 Santa Cruz de La Palma, Tenerife, Canary Islands*
[5] *Royal Greenwich Observatory, Madingley Road, Cambridge CB3 0EZ*
[6] *Planetary Science Institute, 2421 E. 6th Street, Tucson, AZ 85719, USA*
[7] *Department of Physics, University of Tokyo, 7-3-1 Hongo, Bunkyo-ku, Tokyo, Japan*

Accepted 1992 April 15. Received 1992 April 14; in original form 1992 February 28


## SUMMARY

A new intermediate polar (IP) has been found during a programme of optical identification of extreme-ultraviolet sources from the *ROSAT* Wide Field Camera all-sky survey. The new IP, RE0751 + 14, is the first EUV-selected object of its type and only the second such star to have been detected in the extreme ultraviolet. There is evidence that the EUV flux in RE0751 + 14 comes from a soft spectral component which is distinct from the hard X-ray emission. RE0751 + 14 is also unusual in showing a complex modulation profile at the inferred spin period of the white dwarf star, 13.9 min. This is evident both in the infrared, and in the X-ray light curve measured using the *Ginga* satellite. The 13.9-min X-ray light curve is made up of two distinct components which are out of phase: a quasi-sinusoidal modulation which is energy independent, and a narrower 'dip' component which increases in depth towards low energies. These two components may be identified as, respectively, obscuration of the emission region by the white dwarf, and absorption of radiation by the accretion stream. If so, RE0751 + 14 contains elements of both competing models that have been advanced to explain the spin modulation in intermediate polars.


**Key words:** binaries: close – stars: individual: RE0751 + 14 – novae, cataclysmic variables – X-rays: stars.

## 1 INTRODUCTION

The UK Wide Field Camera (WFC) instrument on *ROSAT* has completed the first all-sky survey in the extreme-ultraviolet (EUV) band, between 70 and 200 Å. Many of the EUV sources revealed in the survey have not been catalogued in other wavebands, and we are engaged in a programme of optical identifications using ground-based telescopes to determine the nature of a representative sample of the unidentified WFC survey sources. During the course of this programme we discovered a previously unknown cataclysmic variable (CV) whose EUV emission is designated RE0751 + 14. Further observations of this object reveal it to be a member of the intermediate polar subclass of magnetic CVs, but with some unusual properties.

## 2 WFC DATA

RE0751 + 14 was scanned by the WFC in the interval 1990 October 7–12. It was detected in the short-wavelength scan filter (S1: approximate passband 70–140 Å) at a mean count rate of $0.016 \pm 0.004$ s$^{-1}$. The total exposure time in this filter was 1900 s. The source was not detected in the long-wavelength filter (S2: 110–200 Å) with a 90 per cent upper limit of 0.003 count s$^{-1}$ in a total exposure of 1600 s. The EUV source was located at RA (2000) $7^{\rm h}\,51^{\rm m}\,20\overset{\rm s}{.}4$, Dec. (2000) $+14°\,45'\,10''$ with a 90 per cent confidence error radius of 62 arcsec.

The ratio of counts in the two WFC survey filters, $S1/S2 > 5.5$, is high among sources detected in the WFC survey, and places interesting constraints on the EUV spectrum. We can state with 90 per cent confidence that *S1*/*S2* > 3.2. Hard sources whose low-energy emission is cut off by interstellar absorption do not yield such high ratios. This is because the S2 filter has an X-ray leak which extends to higher energies than the S1 bandpass (Wells *et al.*, in preparation). A high S1/S2 ratio can only come about if the source spectrum is both very soft and cut off by absorption. The high ratio in RE0751 + 14 is evidence that the WFC is detecting a distinct soft emission component in the source, and not the low-energy tail of a hard X-ray spectrum.

## 3 FOLLOW-UP OBSERVATIONS

RE0751 + 14 was identified as a CV spectroscopically using the Faint Object Spectrograph (FOS) on the 2.5-m Isaac Newton Telescope (INT) on La Palma. Subsequently, time-series observations of the star were made in the infrared, using the UK Infrared Telescope (UKIRT) on Mauna Kea, and in the optical using the 1.0-m Jacobus Kapteyn Telescope (JKT) on La Palma. Time-resolved spectroscopic observations were made using the William Herschel (WHT) and INT telescopes on La Palma, and the 1.8-m Perkins telescope at Lowell Observatory, Arizona. The source was also observed with the *Ginga* X-ray satellite. The observations are discussed in detail in subsequent sections. A summary of the observations is contained in Table 1.

### 3.1 Optical identification

The RE0751 + 14 field was observed with the INT FOS on 1991 January 17. The EUV error box is superposed on the optical field in Fig. 1. The latter is derived from a digitized scan of the blue (O) first-epoch POSS plate, made with the PDS at the Royal Greenwich Observatory, Cambridge. Star 1 is the cataclysmic variable believed to be the origin of the EUV emission. Its position, measured from the PDS scans, is RA (2000) $7^h\,51^m\,17\overset{s}{.}3$, Dec. (2000) + 14° 44′ 23″. The calibrated FOS spectrum of star 1 is displayed in Fig. 2 and shows prominent Balmer emission lines, together with lines of He I and He II, superposed on a blue continuum. The *V* magnitude of the star estimated from the spectral flux at 5500 Å is 14.5.

Stars 2 and 3 in Fig. 1 were also observed with the FOS. Both were found to be normal F–G stars.

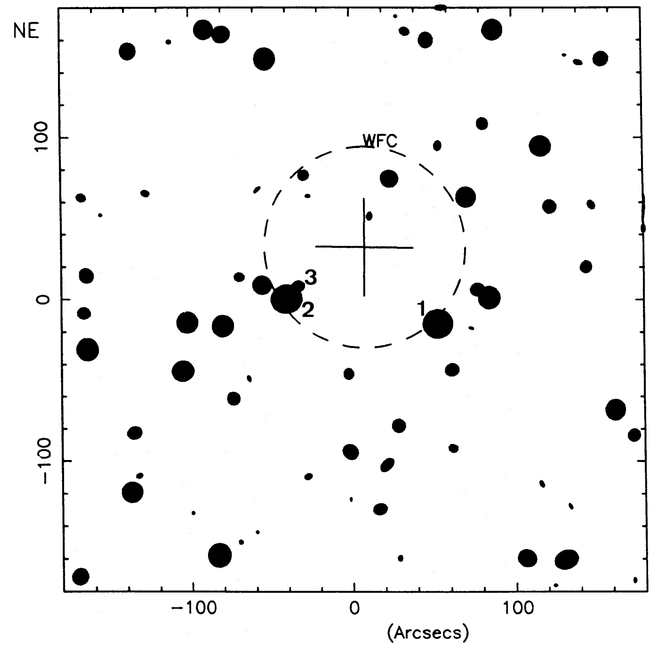


**Figure 1.** Finding chart derived from a PDS scan of the blue (O) first-epoch POSS plate. The WFC error circle is superposed, and the stars observed in the ID programme are numbered. Star 1 is the cataclysmic variable. Its position is RA(2000) $07^h\,51^m\,17\overset{s}{.}3$, Dec.(2000) + 14° 44′ 23″.

**Table 1.** Observation summary.

| Observation Type | Telescope | Instr. | Waveband | UT Date (1991) (unless stated) | Time Res. | Observer |
|---|---|---|---|---|---|---|
| EUV | *ROSAT* | WFC | 70-140Å, 110-200Å | 1990 Oct 7 – Oct 12 | 100m | |
| Spectroscopy | INT | FOS | 3600-10,000Å | Jan 17 | – | Opt.ID |
| IR Fast Photometry | UKIRT | UKT9 | K +(J,H) | Feb 08 09:10 – 08 13:20 | 10s | KOM |
| Optical Photometry | JKT | CCD Camera | V | Jan 26 01:58 – 26 03:48 | 128s | DHPJ |
| | | | | Jan 26 23:09 – 27 00:51 | 64s | |
| | | | | Jan 27 22:52 – 28 01:11 | 64s | |
| | | | | Jan 28 02:12 – 28 03:27 | 64s | |
| | | | | Feb 22 01:07 – 22 03:12 | 64s | |
| Optical Spectroscopy | WHT | ISIS | 4000-5000Å 6200-6800Å | Jan 22 01:33 – 22 03:20 | 5m | PAC |
| | INT | IDS/CCD | | Feb 27 21:20 – 28 03:35 | 5m | (service) |
| | Perkins | CCD | 4000-5000Å | Mar 18 03:05 – 18 07:12 | 5m | SBH |
| X-ray | *Ginga* | LAC | 2-30 keV | (April 15), May 4-5 | 10s | |

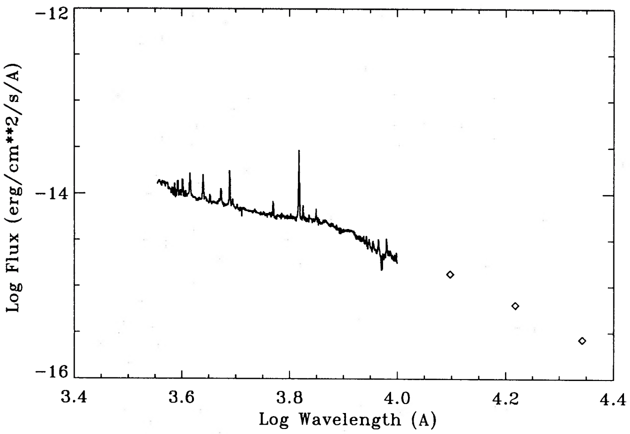


**Figure 2.** Spectrum of RE0751 + 14 star 1 taken with the FOS on the INT. The diamonds are fluxes in the infrared derived from broad-band measurements made in *J*, *H* and *K* filters using the UKT9 photometer on UKIRT. There could be a slight normalization shift ( ~ 10 per cent) between the optical and infrared data due to the imperfect calibration of the FOS spectrum, coupled with the fact that the optical and infrared data are not simultaneous.

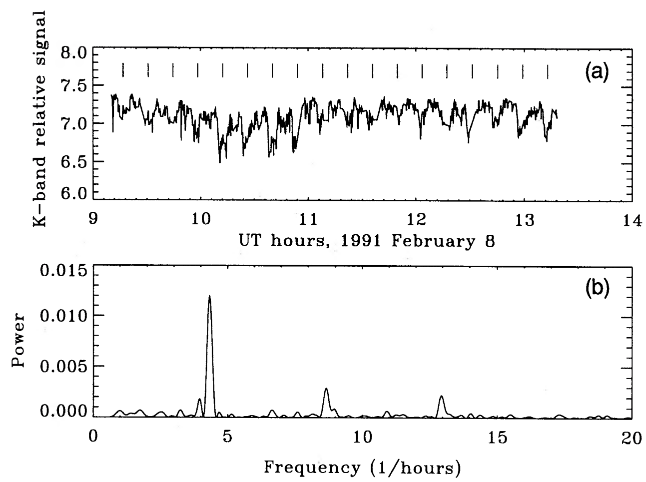


**Figure 3.** (a) Time-series data on RE0751 + 14 in the *K* band taken with the UKT9 photometer on UKIRT. The time resolution is 10 s. A three-point running median filter has been applied to the data before plotting. The 13.9-min periodic variation is apparent in the data; tick marks indicate the times of minimum. (b) Power spectrum of the data in (a) with a low-order polynomial removed.

### 3.2 Infrared observations

RE0751 + 14 star 1 was observd with the UKIRT telescope on 1991 February 8 using the UKT9 aperture photometer. A series of *J*, *H* and *K* measurements was made initially, along with measurements of flux calibration stars. This was followed by a time series in the *K* band which lasted for about 4 hr and had a time resolution of 10 s.

The three-colour photometry yielded a *K* magnitude of 12.90 with $H-K = 0.19$ and $J-H = 0.24$. These *J*, *H* and *K* flux points are included in Fig. 2. They demonstrate that the break in the slope of the FOS spectrum at about 7000 Å is real; between 7000 and 22000 Å the spectrum can be represented by a power law with a slope of $\sim -2.9$ in $F_\lambda$, whereas the mean slope below 7000 Å is about $-1$.

The *K*-band time-series data are illustrated in Fig. 3(a). The overall trend of the data is flat, apart from a broad dip which has a depth of about 5 per cent of the mean level and is centred at about 10:20 UT. However, the data exhibit apparently periodic variations on a time-scale of ~ 15 min that are much larger than can be accounted for by measurement uncertainty. A power spectrum of the (detrended) *K*-band data confirms this, as is shown in Fig. 3(b). There is a strong peak in the power spectrum at a period of 13.9 min, with significant power also at the harmonics of this period. There is also a lesser peak in the power spectrum at a period of 15.2 min, just longward of the 13.9-min periodicity. The power in the 13.9-min peak corresponds to a mean pulse fraction of 0.015. In Fig. 3(a), though, we see evidence that the apparent amplitude of the 13.9-min pulse changes with time, being particularly high during the dip in the light curve at about 10:20 UT, and again towards the end of the observation. The time-scale for this long-term change in pulse amplitude is consistent with the separation in frequency of the 13.9-min peak from the peak at ~ 15.2 min, and it is possible that interference between the two variations is the cause of the long-term modulation. It may also not be coincidental that the separation of the 13.9- and 15.2-min peaks (giving a beat period of ~ 2.7 hr) is consistent with half the (poorly determined) orbital period of the system (see Section 3.4).

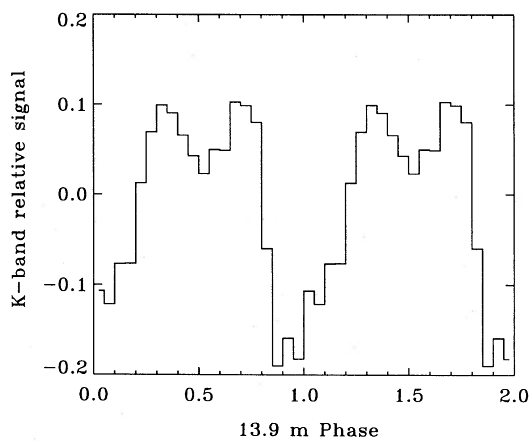


**Figure 4.** *K*-band data of Fig. 3 folded into 20 bins on the 13.9-min period. Two cycles are shown for clarity.

The detrended *K*-band data are folded on the 13.9-min period in Fig. 4. The light curve is clearly not sinusoidal, but has two unequal minima, consistent with the harmonic structure seen in the power spectrum.

### 3.3 Optical CCD photometry

Star 1 was observed in the *V* band with the CCD camera on the JKT telescope on three consecutive nights between 1991 January 26 and 28 and also on 1991 February 22. Three of the runs were comparatively short ( ~ 2 hr) while the fourth (on January 27/28) spanned 4.5 hr with a gap of 1 hr during the run. The integration time was 64 s except for the first run, on January 26, when it was 128 s. Conditions were not completely photometric, and the brightness of star 1 was measured relative to other stars in the CCD frame.

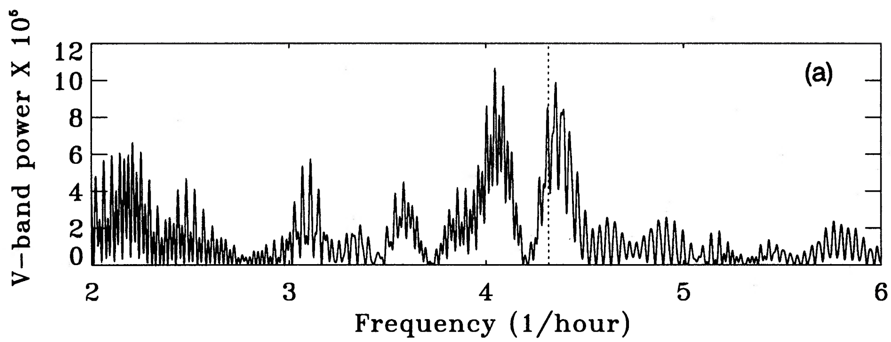


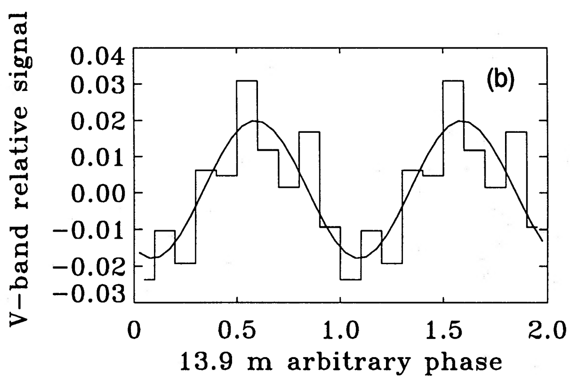


**Figure 5.** (a) Power spectrum of *V*-band CCD photometry taken between 1991 January 26 and 28. The 13.9-min period of the source is marked as a dotted line. (b) Data of January 28 folded on the 13.9-min period. The cycle is divided into 10 bins, and two cycles are shown for clarity.

Fig. 5(a) shows part of a power spectrum of the combined data from the January 26–28 CCD runs. The power spectrum is highly structured because of the strong 1-d aliases in the data. There is significant power at a frequency corresponding to the 13.9-min period identified in the infrared data; the exact infrared period is marked in the figure, and coincides with the second highest of the diurnal alias peaks. There is also significant power centred at about 14.8 min. This is reminiscent of the second (15.2-min) peak in the infrared power spectrum, though at face value the two periods are not consistent.

The data of January 27/28 are folded on the infrared period in Fig. 5(b). This shows a quasi-sinusoidal light curve which has a pulse fraction of 0.02 (*cf.* a pulse fraction of 0.015 for the *K*-band data). To make a more precise estimate of the 13.9-min period, we have fitted sinusoids to each set of CCD data in turn, and also to the *K*-band data of Section 3.2. The short January 26 and 27 data sets were combined for this purpose, to improve statistical quality. The heliocentric epochs of maximum of the fitted sinusoid are listed in Table 2, together with the inferred relative cycle count, *N*. These yield the following ephemeris for the 13.9-min modulation:

$$T_{\max} = \text{HJD } 2448295.9425 \pm 0.0007 + N \times 0^{\mathrm{d}}.0096495 \pm 0^{\mathrm{d}}.0000002,$$

where $T_{\max}$ is the time of maximum of the fitted sinusoid. In addition to the time-resolved *V*-band photometry, CCD images in *U*, *B*, *V*, *R* and *I* filters were made on 1991 January 26 and 27. The broad-band fluxes confirm the FOS measurements of 1991 January 17 which are displayed in Fig. 2.

**Table 2.** Maximum of fitted 13.9-min sinusoid.

| Epoch H.J.D. | error | Rel. Cycle Count | Passband |
|---|---|---|---|
| 2448282.6066 | 0.0007 | -1382 | V |
| 2448284.4600 | 0.0003 | -1190 | V |
| 2448295.9427 | 0.0002 | 0 | K |
| 2448309.5578 | 0.0005 | 1411 | V |

The CCD imaging also reveals that star 1 has a faint companion. The companion is 3.9 mag fainter than star 1 in the *V* band, and consequently would contribute 2.5 per cent of the total light if it were not resolved from star 1.

### 3.4 Time-resolved optical spectroscopy

Time-resolved optical spectroscopic observations of star 1 have been made on three occasions, using the WHT and INT telescopes on La Palma, and the Perkins telescope at Lowell Observatory. The star was observed for about 2 hr with the WHT on 1991 January 22, using the ISIS spectrograph which has two independent arms to view the blue and red spectra simultaneously with separate detectors. The IPCS detector was used with the blue arm to record the spectrum between 4000 and 5000 Å, while a CCD detector on the red arm measured the spectrum around H$\alpha$. Further observations of H$\alpha$ were made on 1991 February 28 during a 5.5-hr observation which utilized the IDS spectrograph on the INT,

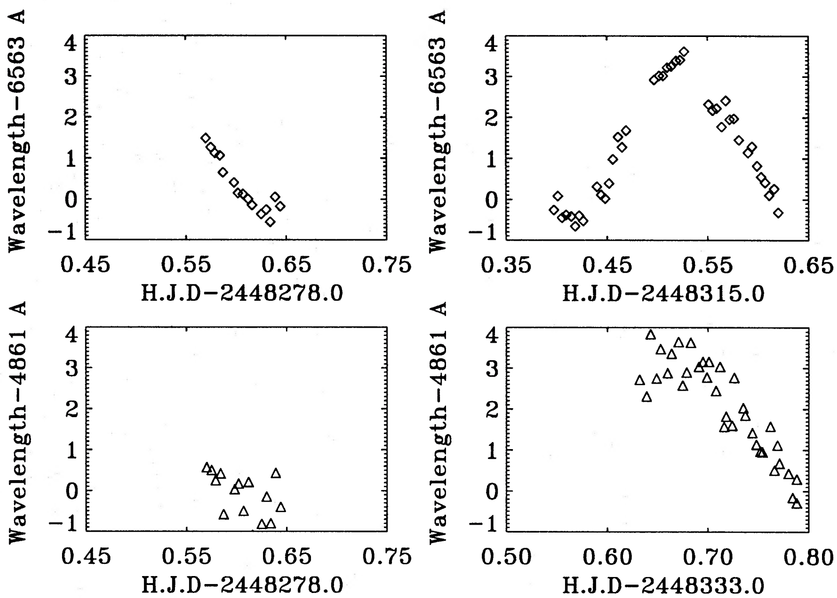


**Figure 6.** The peak wavelength of simple Gaussian profiles fitted to the H$\alpha$ and H$\beta$ emission lines in RE0751 + 14.

coupled with a CCD detector. Finally, the 4000–5000 Å region was observed with the CCD spectrograph on the Perkins telescope on 1991 March 18 over an interval of 4 hr. In all cases an integration time of about 5 min was used.

The emission lines of star 1 are broad, with a FWHM ~ 700 km s$^{-1}$, and show marked profile changes on a time-scale of about an hour. To search for evidence of periodic profile shifts, we have fitted a simple Gaussian profile to the H$\alpha$ or H$\beta$ line in each spectrum, and have plotted the position of the fitted peak as a function of time in Fig. 6. The data are also listed in Table 3. It should be stressed that the line profiles are rarely adequately fitted by a simple Gaussian, and the results should be treated with appropriate caution. However, the Gaussian fits are sensitive to trends in the line shape and velocity, and are a simple and reproducible way to compare our data with future observations for the purposes of period searching.

Fig. 6 demonstrates that there are clear trends in the centroid wavelength of the fitted Gaussian, suggestive of orbital motion. The February data suggest that the spectroscopic period of the source is about the same length as that observation, about 5.5 hr. The other, shorter, observations exhibit variations that are consistent with such a period. Our observing epochs are too widely spaced to allow us to determine a unique period (observations on consecutive nights are needed). However, a period of 5.658 hr provides a consistent description of the data we have in terms of a single periodic motion.

### 3.5 X-ray data

Hard X-ray observations of RE0751 + 14 were made with the *Ginga* Large Area Proportional Counter (LAC; Turner *et al.* 1989) on 1991 April 15, and again on 1991 May 4–5. During the April observation stable pointing was not achieved and less than 1000 s of useful data were obtained. The May observation spans ~30 hr with an effective exposure time of 7.7 hr (*Ginga* coverage is interrupted by occultations of the source by the Earth, and by high-background regions where no useful data are obtained). Both observations were carried out primarily in MPC1 mode at low bit rate, in which 1.2–37 keV spectra are accumulated in 48 spectral channels with a time resolution of 16 s. Subsequent analysis of the X-ray data used the standard background-subtraction procedures utilizing a 'local' background observation made several days after the RE0751 + 14 observation. RE0751 + 14 was detected in both observations with a LAC count rate (2–10 keV) of ~ 10 count s$^{-1}$.

The hard X-ray light curve obtained from the May observation, after background subtraction and correction for attitude variations, is shown in Fig. 7. The light curve shown is for the 4–10 keV X-ray band as, for parts of the observation, the data below ~4 keV are contaminated by solar X-rays. Fourier analysis of the X-ray light curve demonstrates that there is a highly significant modulation with a 13.9-min period; indeed this modulation can be clearly seen in the time-series data (see inset to Fig. 7). This confirms the infrared and optical results and also confirms the identification of star 1 with the source of the EUV/X-ray signal. Fig. 8 shows the raw power spectrum for the 4–10 keV energy range, together with the CLEANed power spectrum obtained by using the CLEAN algorithm (Roberts, Lehár & Dreher 1987, as implemented by Lehto 1989) which successfully removes almost all the window function artefacts which arise from the *Ginga* sampling. The only significant power appears at the fundamental and harmonics of the 13.9-min period. There is no evidence for any significant signal at the ~15-min period seen in the optical and infrared, nor for any significant modulation at any period of the order of 5–6 hr (the likely orbital period of this system).

Fig. 9 shows the X-ray data folded at the 13.9-min period, with an arbitrary phase origin. For the data above 6 keV the whole data set has been used, whilst in the 2–6 keV range the data have been filtered to remove those time periods affected

**Table 3.** Gaussian fits to H$\alpha$ and H$\beta$.

| H.J.D. 2448000+ | $\lambda_{peak}$ Å | H.J.D. 2448000+ | $\lambda_{peak}$ Å | H.J.D. 2448000+ | $\lambda_{peak}$ Å |
|---|---|---|---|---|---|
| 278.570 | 6564.48 | 315.397 | 6562.74 | 333.632 | 4863.72 |
| | 4861.57 | 315.401 | 6563.08 | 333.639 | 4863.31 |
| 278.575 | 6564.26 | 315.405 | 6562.55 | 333.643 | 4864.84 |
| | 4861.50 | 315.409 | 6562.62 | 333.649 | 4863.75 |
| 278.579 | 6564.12 | 315.414 | 6562.58 | 333.653 | 4864.47 |
| | 4861.25 | 315.418 | 6562.34 | 333.660 | 4863.88 |
| 278.584 | 6564.06 | 315.422 | 6562.60 | 333.664 | 4864.36 |
| | 4861.42 | 315.426 | 6562.47 | 333.671 | 4864.65 |
| 278.587 | 6563.65 | 315.440 | 6563.31 | 333.675 | 4863.58 |
| | 4860.42 | 315.444 | 6563.11 | 333.679 | 4863.90 |
| 278.598 | 6563.40 | 315.448 | 6563.02 | 333.683 | 4864.63 |
| | 4861.03 | 315.452 | 6563.39 | 333.691 | 4864.04 |
| 278.602 | 6563.14 | 315.456 | 6563.98 | 333.695 | 4864.16 |
| | 4861.17 | 315.461 | 6564.52 | 333.699 | 4863.78 |
| 278.607 | 6563.12 | 315.465 | 6564.27 | 333.701 | 4864.16 |
| | 4860.50 | 315.469 | 6564.68 | 333.708 | 4863.45 |
| 278.612 | 6563.00 | 315.497 | 6565.92 | 333.712 | 4864.04 |
| | 4861.21 | 315.502 | 6566.02 | 333.716 | 4862.57 |
| 278.616 | 6562.85 | 315.506 | 6566.02 | 333.718 | 4862.82 |
| | 4859.91 | 315.510 | 6566.22 | 333.724 | 4862.60 |
| 278.625 | 6562.63 | 315.514 | 6566.25 | 333.726 | 4863.77 |
| | 4860.18 | 315.519 | 6566.39 | 333.735 | 4863.03 |
| 278.630 | 6562.74 | 315.523 | 6566.41 | 333.737 | 4862.85 |
| | 4860.85 | 315.527 | 6566.62 | 333.744 | 4862.42 |
| 278.634 | 6562.44 | 315.551 | 6565.32 | 333.748 | 4862.14 |
| | 4860.20 | 315.555 | 6565.17 | 333.752 | 4861.97 |
| 278.639 | 6563.05 | 315.559 | 6565.22 | 333.754 | 4861.95 |
| | 4861.43 | 315.564 | 6564.77 | 333.762 | 4862.58 |
| 278.644 | 6562.82 | 315.568 | 6565.41 | 333.766 | 4861.51 |
| | 4860.60 | 315.572 | 6564.95 | 333.769 | 4862.12 |
| | | 315.576 | 6564.97 | 333.771 | 4861.68 |
| | | 315.581 | 6564.45 | 333.780 | 4861.43 |
| | | 315.590 | 6564.14 | 333.784 | 4860.84 |
| | | 315.594 | 6564.29 | 333.788 | 4860.71 |
| | | 315.599 | 6563.82 | 333.788 | 4861.29 |
| | | 315.603 | 6563.55 | | |
| | | 315.607 | 6563.41 | | |
| | | 315.611 | 6563.10 | | |
| | | 315.616 | 6563.26 | | |
| | | 315.620 | 6562.68 | | |

by solar contamination (unfortunately this amounts to about 68 per cent of the observation).★ The modulation profile is complex and shows a clear dependence on X-ray energy. At the lowest energies there are two maxima and minima per cycle and the profile is highly asymmetric. At higher energies the profile becomes simpler with only one clear maximum and minimum for the data above 10 keV. The phase of maximum flux migrates to earlier values as the energy increases. The full modulation depth at the lowest energies is ~70 per cent, but it is still ~30 per cent above 10 keV. As with the infrared data, there is evidence that the pulse shape changes on time-scales of hours.

★We have verified that the shape of the low-energy pulse is insensitive to the procedure which removes the solar contamination, by comparing the profiles before and after the contaminated intervals were removed. The background level varies with the *Ginga* Earth-orbital period, but this is randomly phased with respect to the 13.9-min period of RE0751+14. Thus the net effect of the contamination is to add a constant level to the folded light curve.

## 4 DISCUSSION

The strong 13.9-min flux modulation of RE0751+14 coupled with the evidence for a ~6-hr orbital period, and the characteristics of the optical spectrum, mark this out as a probable new member of the intermediate polar (IP) subclass of magnetic cataclysmic variable, a grouping which includes less than a dozen confirmed members (e.g. Hellier & Mason 1990). In an IP, periodic flux modulation is associated with the spin period of a magnetized white dwarf or, in some cases, the beat between the orbital and spin periods.

### 4.1 EUV emission

RE0751+14 is so far the only new IP discovered in the *ROSAT* Wide Field Camera survey. Indeed, among the previously known IPs, only EX Hya was detected by the WFC, which suggests that observable EUV emission is rare among this type of CV. This contrasts strongly with the class of phase-locked magnetic CVs, the AM Her stars, where a bright EUV spectral component is seen in the majority of members. Even in EX Hya, it is not clear whether the emission detected by the Wide Field Camera is a distinct spectral component, or merely the unabsorbed extension of the hard X-ray emission, since the ratio of counts in the S1 and S2 filters for this star is approximately 1. As argued in Section 2, the extreme filter ratio in RE0751+14 is suggestive of an EUV emission component distinct from the hard X-ray spectrum in this star.

The EUV emission in AM Her stars is believed to arise from the surface of the white dwarf beneath the accretion column. This accretion footprint is heated to temperatures of order 10 eV by radiant and mechanical energy from the column. The temperature of the emission is determined by the size of the accretion region on the white dwarf, and the amount of energy deposited there (which in turn is related to the accretion rate). A similar EUV spectral component would be expected in IPs if the accretion occurs on to a small enough fraction of the white dwarf's surface (King & Lasota 1990), especially since the observed mean orbital period of the IP group and therefore the expected mean accretion rate are higher than for the AM Her stars.

The detectability of such a component is, however, critically dependent on its temperature and on the amount of interstellar absorption. The absence of detectable soft components in the majority of IPs may simply be due to the fact that the accreting area is larger in IPs than in AM Her stars, and the temperature of the emission too low for it to be detected. This would be exacerbated by a higher interstellar absorbing column, such as might occur on average if the space density of IPs were lower than that of AM Her stars. For example, an equivalent hydrogen column density of only $3\times10^{20}$ cm$^{-2}$ will absorb 90 per cent of the flux emitted at 0.17 keV, the highest energy covered by the WFC, and the absorption rapidly increases towards lower energies.

Conversely, the detection of a soft component in RE0751+14 may suggest that the accretion stream is unusually collimated in that star, or that the absorbing column is unusually low. In this regard, it is interesting to note that RE0751+14 is observed in a direction that was identified by Paresce (1984) as having a very low absorbing column in the vicinity of the Sun.

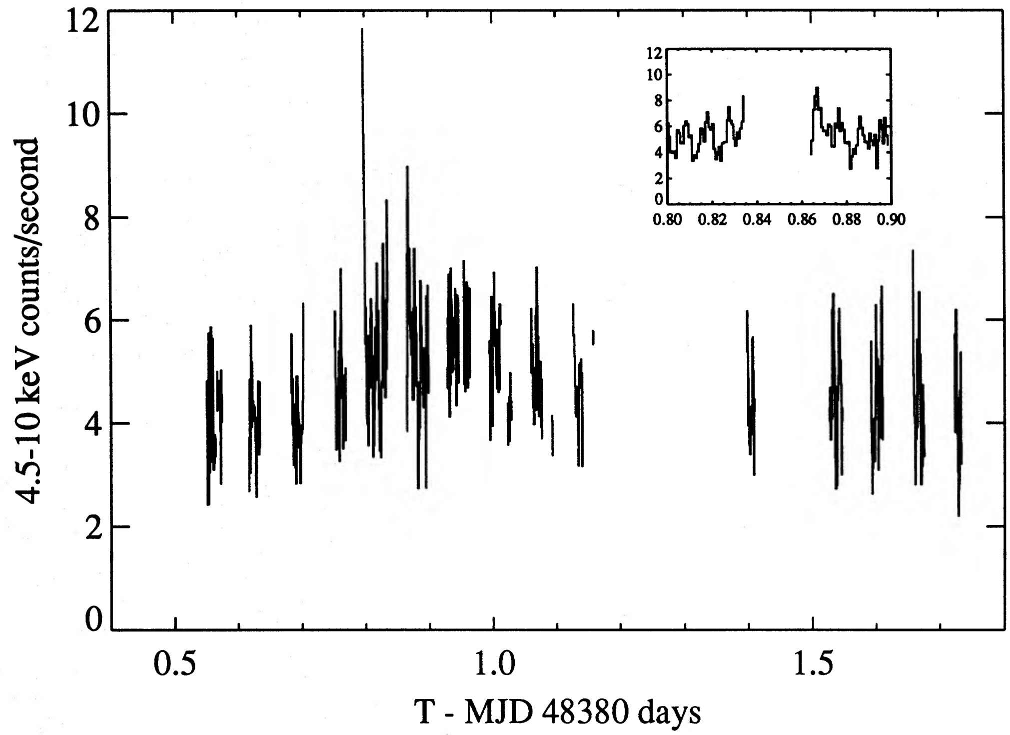


**Figure 7.** The 4.5–10 keV light curve of RE0751 + 14 obtained on 1991 May 4–5 with the *Ginga* satellite. The inset is an expanded view of part of the data in which individual pulses in the 13.9-min modulation can be clearly discerned. MJD is defined as JD − 2400000.5.

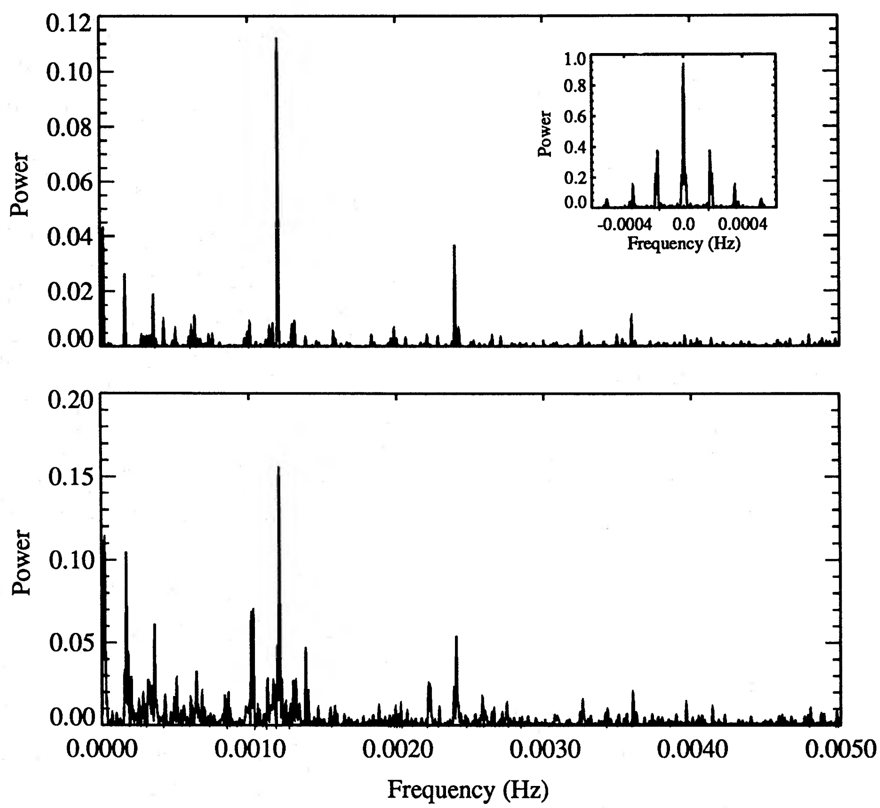


**Figure 8.** The power spectrum of the *Ginga* data. The lower panel shows the raw power spectrum, while the upper panel shows the spectrum after processing using CLEAN to remove window artefacts. The window spectrum is illustrated in the inset. There are prominent peaks in the power spectrum corresponding to the fundamental and harmonics of the 13.9-min modulation.

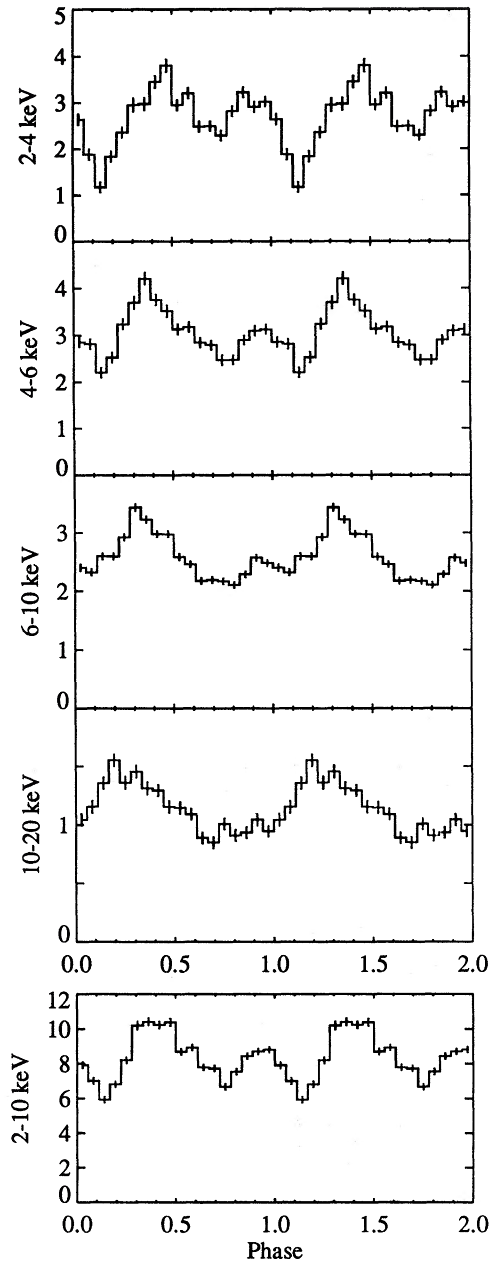


**Figure 9.** The *Ginga* data separated into different wavebands and folded on the 13.9-min modulation period. Periods of contamination by solar X-rays have been removed from the 2–4 and 4–6 keV data, and also the 2–10 keV summary, before folding. The effect of the contamination is to apply a constant offset to the light curve, but it does not affect the shape. The phasing of these data is arbitrary.

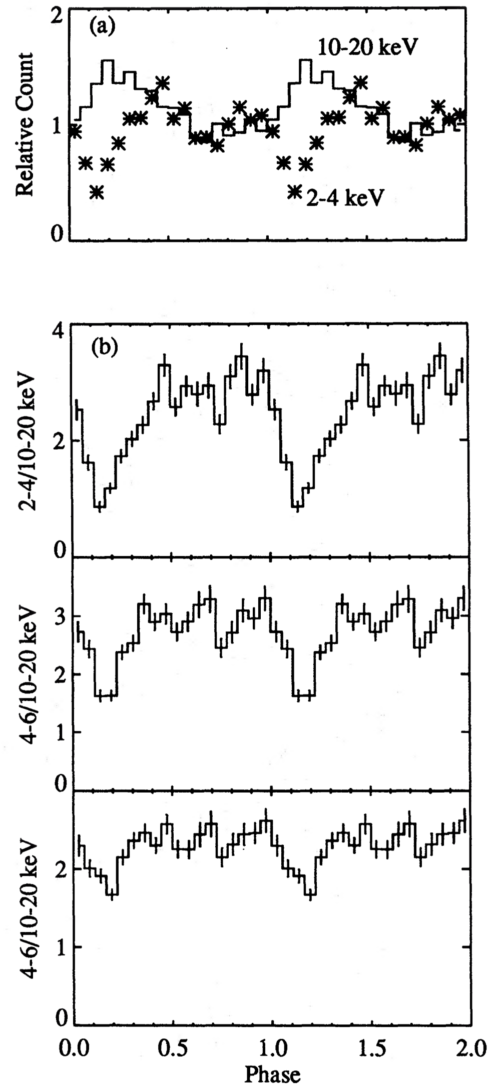


**Figure 10.** (a) A comparison of the 2–4 and 10–20 keV folded data, normalized in the phase region 0.5–1.0. (b) The folded data in various energy bands divided by the pulse profile in the 10–20 keV band to illustrate the shape and energy dependence of the 'dip' component of the modulation (see text). The phase convention in this figure is arbitrary, but consistent with Fig. 9.

### 4.2 The 13.9-min pulsation

RE 0751 + 14 exhibits a complex pulsation light curve, both in the low-energy end of the *Ginga* range (2–10 keV) and in the infrared. Our optical CCD photometry shows no evidence for a departure from a sinusoidal pulse, but the relatively coarse time resolution of the CCD data means that a secondary dip of the kind seen in the infrared would have been difficult to detect. It is important to check whether the secondary dip is present in the optical band, since the overall optical–infrared spectrum (Fig. 2) suggests that the $V$ and $K$ bands may be sampling different emission components.

The complex nature of the 13.9-min pulse profile in RE 0751 + 14 sets it apart from other IPs that have been studied. Generally, the pulse profiles of IPs in the X-ray and optical bands are quasi-sinusoidal, with one maximum and one minimum per cycle (e.g. Patterson & Steiner 1983; Norton & Watson 1989; Rosen *et al.* 1991). The only exception to this statement to date, other than RE 0751 + 14, is for the X-ray light curve of FO Aqr (Norton *et al.* 1992) which, in high-quality data taken with the *Ginga* satellite, is found to exhibit a narrow energy-independent dip in its 20.9-min pulsation light curve, superimposed on the usual energy-dependent, quasi-sinusoidal modulation. The behaviour of FO Aqr is very different to that of RE 0751 + 14, however, and the peculiar nature of the X-ray modulation in

RE0751+14 would have been apparent in much lower quality data than were required to show up the structure in the FO Aqr pulse profile.

To understand the X-ray pulsation light curve of RE0751+14, it is useful to compare the folded 2–4 and 10–20 keV data, as in Fig. 10(a). In this figure, the two curves have been normalized in the phase region 0.5–1.0. The 2–4 keV modulation can be understood as having the same underlying shape as the high-energy modulation but with an extra dip component centred at about phase 0.15. The fact that this dip is most prominent at low energies suggests that it is caused by photoelectric absorption. This is borne out by phase-resolved spectral fits which are consistent with a single absorption column at all phases except during the dip, where the column density derived from a simple model increases. The shift in the time of flux maximum to later phases at low energies can be understood as the effect of the absorption dip progressively cutting into the underlying modulation.

On the assumption that this description is correct, we have divided each of the 2–4, 4–6 and 6–10 keV pulse profiles by the 10–20 keV data (which show no evidence for the absorption dip) in order to display more clearly the energy dependence of the 'dip' component. This is shown in Fig. 10(b). The change in the depth of the dip as a function of energy is not steep enough to be explained as photoelectric absorption by a single uniform column of cold cosmic-abundance material, but may be consistent with absorption in a clumpy medium.

Two main kinds of mechanism have been proposed to explain the X-ray flux modulation in IPs. In the first, the visible fraction of a large emission region, which is offset from the rotation axis of the white dwarf, is modulated as the white dwarf spins (King & Shaviv 1984). Originally envisaged as a filled cap centred on the magnetic pole of the white dwarf, this idea can be extended to include arc- or ring-shaped emission regions. In the second kind of model, the flux is modulated by absorption in the accretion column as the latter moves across the line of sight (Rosen, Mason & Córdova 1988). In this 'accretion curtain' model, material accretes along a semicircular arc offset from the magnetic pole.

Elements of both models can be seen in RE0751+14. The underlying, energy-independent modulation can be understood as part of the emission region passing behind the limb of the white dwarf, while the absorption dip, which is approximately 180° out of phase with the energy-independent component, occurs when the accretion column passes across the line of sight. In comparison with the absorption-related modulations seen in other IPs (e.g. EX Hya: Rosen *et al.* 1988) the absorption 'dip' in RE0751+14 is relatively narrow. This may reflect differences in magnetic field strength, geometry or viewing angle. Asymmetries in both components of the RE0751+14 modulation, on the other hand, could be related to the distribution of material along the accretion arc.

The complex nature of the infrared (and perhaps optical) modulation in RE0751+14 may also be a reflection of the combined effects of occultation and absorption/scattering. Relating the optical/IR and X-ray modulations could shed considerable light on the way in which the optical/IR continuum modulation is produced in IPs. However, we do not yet have sufficient data to compare accurately the phases of the pulsation light curve of RE0751+14 in the two bands.

Another important test of the suggested model for RE0751+14 will be to examine time-resolved spectroscopy of the optical emission lines. Similar studies of other IPs have related the velocity modulation in the lines to the direction of the accretion flow (Hellier *et al.* 1987; Hellier, Mason & Cropper 1990; Hellier, Cropper & Mason 1991), and it should be possible by these means to determine whether the geometry we suggest for RE0751+14 is correct.

## 5 CONCLUSION

In the context of our current knowledge of intermediate polars, RE0751+14 exhibits a number of novel features. These include evidence for a separate soft X-ray/EUV spectral component, and a complex spin pulse profile. We have interpreted the X-ray spin profile as a combination of occultation by the white dwarf and absorption by the accretion stream, an explanation that may be easily testable, particularly by phase-resolved optical spectroscopy. Our interpretation combines the essential elements of what have previously been regarded as two rival models to explain the spin modulation in IPs (e.g. Hellier *et al.* 1991; Norton *et al.* 1992). Detailed study of the absorption and occultation mechanisms in the *same* system, RE0751+14, may well shed light on which of these two effects dominates in other IP light curves. There are also indications of sideband pulsations in the optical and infrared light curves of RE0751+14, and for structure in the optical–infrared continuum. These clearly merit further study. All these features lead us to suspect that RE0751+14 may become a key system in furthering our knowledge of the intermediate polar cataclysmic variables.

## ACKNOWLEDGMENTS

The *ROSAT* Wide Field Camera project is supported by the UK Science and Engineering Research Council. The WFC was developed by a consortium of five UK institutes: the University of Birmingham, the University of Leicester, the Mullard Space Science Laboratory of University College London, the Imperial College of Science and Technology, London, and the SERC's Rutherford Appleton Laboratory. KOM thanks France Córdova, Liz Puchnarewicz and Rick Thomson for allowing him to observe RE0751+14 while their main observing programme was suspended due to instrument problems, the UKIRT night assistant, Joel Aycock, for his persistence in getting UKT9 to work on an off day, and Kevin Krisciunas for assistance in extracting and analysing the data. The Isaac Newton Group of telescopes is operated by the Royal Greenwich Observatory at the Spanish Observatorio del Roque de Los Muchachos of the Instituto de Astrofisica de Canarias. Planetary Science Institute is a division of SAIC.

## REFERENCES

Hellier, C. & Mason, K. O., 1990. In: *Accretion-Powered Compact Binaries,* p. 185, ed. Mauche, C. W., Cambridge University Press, Cambridge.

Hellier, C., Mason, K. O. & Cropper, M. S., 1990. *Mon. Not. R. astr. Soc.,* **242,** 250.
Hellier, C., Cropper, M. S. & Mason, K. O., 1991. *Mon. Not. R. astr. Soc.,* **248,** 233.
Hellier, C., Mason, K. O., Rosen, S. R. & Córdova, F. A., 1987. *Mon. Not. R. astr. Soc.,* **228,** 463.
King, A. R. & Shaviv, G., 1984. *Mon. Not. R. astr. Soc.,* **211,** 833.
King, A. R. & Lasota, J. P., 1990. *Mon. Not. R. astr. Soc.,* **247,** 214.
Lehto, H. J., 1989. *PhD thesis,* University of Virginia.
Norton, A. J. & Watson, M. G., 1989. *Mon. Not. R. astr. Soc.,* **237,** 853.
Norton, A. J., Watson, M. G., King, A. R., Lehto, H. J. & McHardy, I. M., 1992. *Mon. Not. R. astr. Soc.,* **254,** 705.
Paresce, F., 1984. *Astr. J.,* **89,** 1022.
Patterson, J. & Steiner, J. E., 1983. *Astrophys. J. Lett.,* **264,** L61.
Roberts, D. H., Lehár, J. & Dreher, J. W., 1987. *Astr. J.,* **93,** 968.
Rosen, S. R., Mason, K. O. & Córdova, F. A., 1988. *Mon. Not. R. astr. Soc.,* **231,** 549.
Rosen, S. R., Mason, K. O., Mukai, K. & Williams, O. R., 1991. *Mon. Not. R. astr. Soc.,* **249,** 417.
Turner, M. J. L. *et al.,* 1989. *Publs astr. Soc. Japan,* **41,** 345.